Int. J. Heat Mass Transfer. Vol. 20, pp. 763–771. Pergamon Press 1977. Printed in Great Britain

THE EFFECT OF FREE STREAM TURBULENCE LEVEL ON THE FLOW AND HEAT TRANSFER IN THE ENTRANCE REGION OF AN ANNULUS

M. R. F. HEIKAL, P. J. WALKLATE and A. P. HATTON
Department of Mechanical Engineering, University of Manchester Institute of Science and Technology, Manchester, M60 1QD, U.K.

(*Received* 13 *July* 1976 *and in revised form* 28 *October* 1976)

Abstract—Measurements were made of turbulence characteristics, mean flow and heat-transfer parameters in the entrance region of an annulus of radius ratio 0.25 over a range of Reynolds numbers from 0.13×10^5 to 1.9×10^5. Tests were carried out with and without a turbulence promoter which gave a large enhancement of free stream turbulence at inlet. The results were compared using a prediction method based on the two equation turbulence model. Good agreement was obtained both in the entrance region and the fully developed situation and with and without the turbulence promoter providing proper values of the initial turbulence energy and dissipation rate were used.

NOMENCLATURE

A, B, C, hot-wire calibration constants;
C_1, C_2, C_3, C_m, turbulence model constants;
C_f, coefficient of friction;
C_p, specific heat;
D_e, equivalent diameter, $= 2r_e$;
e, e', hot-wire voltage and fluctuation in voltage;
E, dimensionless rate of dissipation of turbulence energy, $= \frac{\nu^2}{u_b^4}\left[\frac{\partial u_j'}{\partial x_k}\right]^2$;
k, turbulence kinetic energy, $= \frac{\overline{u'^2}+\overline{v'^2}+\overline{w'^2}}{2}$;
K, mixing length constant;
Nu, Nu_∞, local and fully developed Nusselt number;
P, pressure;
Pr, Prandtl number;
q, heat flux;
Q, dimensionless turbulence kinetic energy, k/u_b^2;
r, r_e, radius and equivalent radius, $r_e = r_o - r_i$;
R, dimensionless stream function, $= \int_{r_1}^{r_o} \frac{ur\,dr}{\nu r_e} - \int_0^x \frac{vr\,dx}{\nu r_e}$;
t, temperature;
T, dimensionless temperature, $T = \frac{(t-t_{in})}{q_i/\rho C_p u_b}$;
u, u_b, u', local, bulk mean and fluctuating component of axial velocity;
U, effective cooling velocity in hot-wire analysis;
v, v', local and fluctuating component of radial velocity;
w, w', local and fluctuating component of tangential velocity;
x, distance along the annulus;
X, non-dimensional distance along the annulus, $= \int_0^x \frac{u_b\,dx}{\nu}$;
y, distance from the wall: for outer layer $y = r_o - r$; for inner layer $y = r_i - r$;
y^+, dimensionless distance from the wall, $= \frac{y[\tau_w/\rho]^{\frac{1}{2}}}{\nu}$;
Z, dimensionless velocity, $= \frac{u}{u_b}$.

Greek symbols

ε_m, eddy diffusivity of momentum;
$\delta_h, \delta_k, \delta_\varepsilon$, ratios of turbulent diffusivity of momentum to turbulent diffusivities of heat, turbulence energy and dissipation rate of turbulence energy;
ν, kinematic viscosity;
ρ, density;
τ, shear stress.

Subscripts

i, inner boundary layer;
in, inlet value;
j, k, orthogonal space planes;
o, outer boundary layer;
p, position near a wall ($y^+ = 30$) where the Van Driest turbulence model and the turbulence energy–dissipation model are matched;
w, wall position.

1. INTRODUCTION

BECAUSE of its importance in heat exchanger and nuclear reactor design applications the annulus geometry has been subjected to much attention in the past. An important feature, which is different from the plain tube geometry, is that heat may be transferred from one wall to the other and therefore the correct description of the diffusion in the central region is of much greater importance. Most of the past work has been concerned with fully developed flow and even here there are certain questions which still remain unanswered. It is the purpose of this article to present information additional to the limited work which has been done on the flow development in the entrance region. No measurements have been previously made of the turbulence structure in this region or of the effect on the turbulence quantities and the other boundary-layer parameters, such as the displacement and momentum thickness of the level of the stream turbulence at inlet. This effect was an important objective of the experiments to be discussed here.

Apart from its basic importance in practical applications the flow development in the entrance region of an annulus is an interesting case on which to test prediction methods which have been recently proposed.

This case should be an exacting test of such methods since the boundary layers may grow at different rates along the channel and there will probably be a period of readjustment necessary to achieve the fully developed form after the boundary layers have interfered. To allow for the additional parameter of inlet turbulence level presents a further and demanding test of any prediction method.

The prediction methods used were based on the proposals of Spalding and Launder [1]. First a two equation model was used with an eddy diffusivity determined from the solution of the transport equations of turbulence energy and the rate of dissipation of this quantity. However, the programme used was, for historical reasons, developed separately from that described in [1] and it has a number of different features.

In addition, the three equation model proposed by Hanjalic and Launder [2] which included an additional Reynolds stress equation, without involving eddy diffusivity, was used although for the situations considered here there was little difference between the results of the two methods.

2. EARLIER STUDIES ON THE ANNULUS

The annulus has been the subject of much attention, both experimental and theoretical. However, most of the earlier work has been on the fully developed flow situation with particular attention being paid to the value of the radius of zero shear or of the radius of maximum velocity and whether there exists any difference between these positions. The main difficulty in the annulus is to determine the shear stress on the inner and outer surfaces. Smith *et al.* [3] measured the inner shear stress with a floating element and they were able to show the radius of zero shear obtained by this method agreed with that obtained by hot wires. There was a significant difference from the radius of maximum velocity for the annulus radius ratio of 0.088.

Measurements, including Reynolds stresses by hot wire techniques, by Brighton and Jones [4] showed that there was negligible difference between the two positions for radius ratios greater than 0.1. They also showed that the inner velocity profile was different from the universal form of round pipe flow.

Predictions of velocity distributions and heat transfer in annuli by Quarmby and Anand [5] and Kays and Leung [6] showed good agreement with experiment. In both cases the radius of zero shear was assumed the same as that of maximum velocity but the eddy diffusivity variation was not derived from the equations of motion. Instead an empirical correlation based on experiments was used for this quantity. Wilson and Medwell [7] presented a self consistent analysis in which the mixing length variation of Van Driest was applied throughout the flow. They obtained good prediction of friction factor but did not show comparison of their eddy diffusivity predictions with the experimental or theoretical values presented earlier.

An analysis using integral techniques and Reynolds analogy was presented by Roberts and Barrow [8] who also made heat-transfer measurements in the combined hydrodynamic and thermal entrance region. They obtained good agreement and showed that the variation of Nusselt number was not significantly different from the situation where the velocity profile remains unchanged.

More recent work by Hanjalic and Launder [2] has shown that the flow details, including the non-coincidence of the radii of zero shear and maximum velocity, can be predicted by a three equation turbulence model in which the eddy diffusivity concept is not used. In a smooth annulus however of the radius ratio used in the present experiments the two equation model will be shown to give satisfactory predictions.

Some measurements and predictions have been made in the entrance regions of parallel wall channels by Stephenson [9], Hatton and Woolley [10] and in a pipe by Walklate *et al.* [11]. Apart from the latter reference, however, comparisons are made of only mean flow parameters although these were shown to be mainly satisfactory. It was also shown that there is little difference between Stanton numbers for the situations where the velocity profile is developing and where it is unchanging along the duct.

3. APPARATUS

The tests were carried out in an annulus of inner and outer radii 12.7 and 50.8 mm and total length 3.75 m giving an overall length/equivalent diameter ratio of 49. Air was drawn through the annulus by a centrifugal fan to obtain Reynolds numbers in the range $0.13 \times 10^5 - 1.9 \times 10^5$. The air was filtered at inlet before entering a settling chamber from which it passed to the annulus through a mouthpiece shaped to give constant acceleration. For tests in which a high turbulence level was required a turbulence promoter

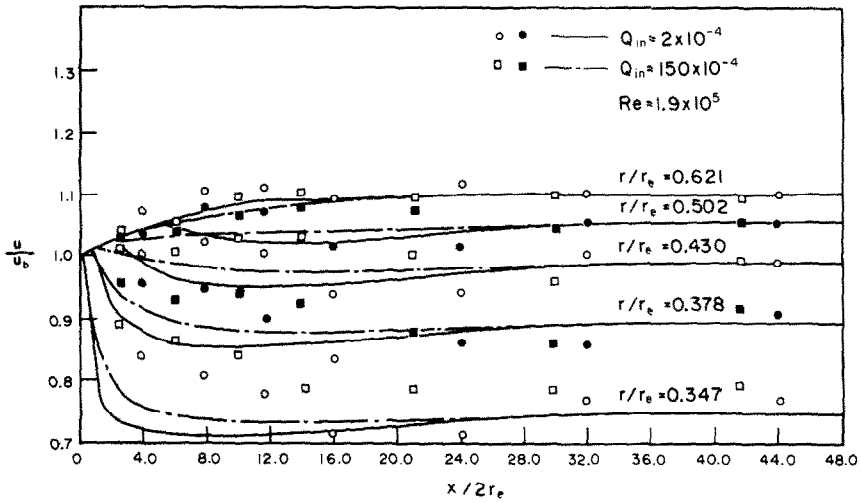

FIG. 1(a). Variation of mean velocity at particular radii along the annulus (inner profile).

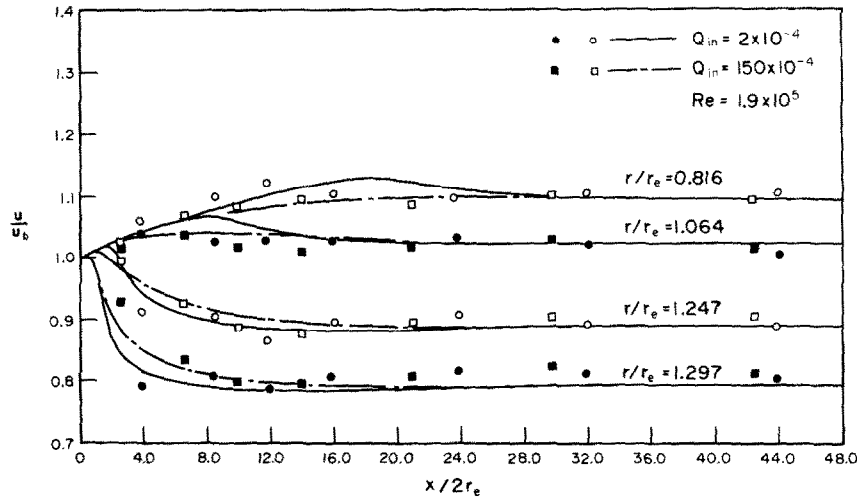

FIG. 1(b). Variation of mean velocity at particular radii along the annulus (outer profile).

was included after the entry section. The promoter consisted of eighteen radial strips at equal angular intervals, the trailing edges of which were saw cut to a depth of 2.4 mm at intervals of 2.4 mm and then bent alternately in opposite directions. This produced a very large enhancement of turbulent energy at the inlet to the annulus.

Standard commercial hot wire equipment was used with wires 1.5 mm long and 0.005 mm dia. Radial traverses were made at a number of locations with single wires, both straight and inclined at 45° and in both vertical and horizontal planes. Traverses using total head and static tubes were also carried out to obtain mean velocity profiles and the usual corrections for turbulence and displacement effects were considered. The Reynolds number was obtained from these traverses and was observed to be closely constant at all the axial stations which provided a check that the flow was axisymmetric.

The central core of wall thickness 2.2 mm was heated electrically and was fitted with thermocouples which were spaced at 2.54 cm intervals near the inlet but at wider spacing further down the duct.

All readings were fed into a computer program which determined all the important parameters including the Reynolds and Stanton numbers. For the latter, corrections were included for axial conduction in the core tube and radiation, both of which were small. The necessary physical properties were taken at the film temperature, i.e. the arithmetic mean of wall and bulk temperatures.

4. HOT WIRE SIGNAL ANALYSIS

The wires were calibrated in a small low turbulence wind tunnel by reference to a pitot tube. The equation described by Davies and Patrick [12] was used to correlate the results and they showed that this form gives a much improved dynamic response equation than the usual King's Law. This equation is:

$$e^2 = A + BU^{\frac{1}{3}} + CU. \quad (1)$$

A least squares second order polynomial of the above

form was used to fit the values e^2 and $U^{\frac{1}{2}}$ obtained from the calibration to obtain A, B and C. Having obtained these constants the velocity was obtained by inverting equation (1) to give:

$$U = \{[-B + [B^2 - 4C(A-e^2)]^{\frac{1}{2}}]/2C\}^2 = \phi(e).$$

Since A, B and C do not vary with U, differentiation of equation (1) leads to an expression for the wire sensitivity

$$\frac{de}{dU} = \frac{2C + BU^{\frac{1}{2}}}{4e} = S \tag{2}$$

and if de and dU are assumed to be equivalent to small fluctuations of voltage e' and velocity U' then:

$$\frac{e'}{U'} = S = \frac{(\overline{e'^2})^{\frac{1}{2}}}{(\overline{U'^2})^{\frac{1}{2}}}. \tag{3}$$

Combining (1), (2) and (3) with $D = B^2 + 4C(e^2 - A)$ the turbulence intensity is given by:

$$\frac{4e(\overline{e'^2})^{\frac{1}{2}}}{\{D - BD^{\frac{1}{2}}/2C\}}. \tag{4}$$

To determine the usual fluctuating components of velocity parallel and normal to the mean flow $\overline{u'^2}$; $\overline{v'^2}$ and $\overline{w'^2}$ and the stress components $\overline{u'v'}$ and $\overline{u'w'}$ it is necessary to make five traverses, one with a wire normal to the mean flow direction, two with the wire in the vertical plane inclined at $\pm 45°$ to the mean flow and two with the wire in the horizontal plane included at $\pm 45°$ to the mean flow. The procedure for analysing the signals is well known and the equations are given for example, in [13]. However, the method used to compensate for the deviation from the "cosine law" was different. In the present work a direct calibration method was used to account for the cooling effect of tangential velocity component. The wire was calibrated at an angle of 45° to the flow direction, and a cosine law was assumed in obtaining the calibration constants. In this way the calibration constants included the effect of the tangential component of the velocity.

5. PREDICTION METHOD

The boundary-layer forms of the equation of momentum and thermal energy were solved numerically in the entrance region using well known techniques. For the flow situation in question (i.e. a duct of specified dimensions) it is necessary to calculate the axial pressure gradient distribution in order to solve for momentum. This was achieved by the continuous correction of an estimated pressure gradient based on the resultant out of balance of the mass flow rate. The procedure used is described by Briley [14] who applied it to a three dimensional parabolic duct flow.

The boundary-layer momentum and energy equation, including the well known eddy diffusivity assumptions and neglecting axial diffusion, may be written:

$$u\frac{\partial u}{\partial x} + v\frac{\partial u}{\partial r} = -\frac{1}{\rho}\frac{\partial p}{\partial x} + \frac{1}{r}\frac{\partial}{\partial r}\left\{r(\nu + \varepsilon_m)\frac{\partial u}{\partial r}\right\}$$

$$u\frac{\partial t}{\partial x} + v\frac{\partial t}{\partial r} = \frac{1}{r}\frac{\partial}{\partial r}\left\{r(\alpha + \varepsilon_h)\frac{\partial t}{\partial r}\right\}.$$

These transform to:

$$\frac{\partial Z}{\partial X} = \frac{-2}{\rho u_b^2}\frac{\partial P}{\partial X} + Z^{\frac{1}{2}}\frac{\partial}{\partial R}\left[\left(\frac{r}{r_e}\right)^2\left[1 + \frac{\varepsilon_m}{\nu}\right]\frac{\partial Z}{\partial R}\right] \tag{5}$$

$$\frac{\partial T}{\partial X} = \frac{\partial}{\partial R}\left[\left(\frac{r}{r_e}\right)^2 Z^{\frac{1}{2}}\left[\frac{1}{Pr} + \frac{\varepsilon_m}{\nu\delta_h}\right]\frac{\partial T}{\partial R}\right] \tag{6}$$

where

$$X = \int_0^x \frac{u\,dx}{\nu} \quad Z = \frac{u^2}{u_b^2}$$

$$R = \int_{r_i}^{r_o} \frac{ur\,dr}{\nu r_e} - \int_0^x \frac{\nu r\,dx}{\nu r_e} \quad T = \frac{t - t_{in}}{q_i/\rho C_p u_b}.$$

The turbulence model to be employed in the prediction method involves the numerical solution of two additional nonlinear partial differential equations for the turbulence kinetic energy k and the rate of dissipation of turbulence kinetic energy $\nu(\overline{\partial u_j'}/\partial x_k)^2$, and was the same as that described by Launder and Spalding [1]. Further, it is postulated that the remaining unknown eddy diffusivity, by dimensional analysis, is given by:

$$\frac{\varepsilon_m}{\nu} = C_m\frac{Q^2}{E} \tag{7}$$

where Q is a dimensionless turbulence kinetic energy k/u_b^2, E is a dimensionless rate of dissipation of turbulence kinetic energy defined as $E = (\nu^2/u_b^4)(\overline{\partial u_j'}/\partial x_k)^2$ and C_m is a constant. The boundary-layer form of the transport equations for Q and E after transformation to X–R co-ordinates are written:

$$\frac{\partial Q}{\partial X} = \frac{\varepsilon_m}{\nu}\frac{1}{4Z^{\frac{1}{2}}}\left[\frac{r}{r_e}\frac{\partial Z}{\partial R}\right]^2 - \frac{E}{Z^{\frac{1}{2}}} + \frac{\partial}{\partial R}\left[\left(\frac{r}{r_e}\right)^2 Z^{\frac{1}{2}}\left[1 + \frac{\varepsilon_m}{\nu\delta_k}\right]\frac{\partial Q}{\partial R}\right] \tag{8}$$

$$\frac{\partial E}{\partial X} = C_1\frac{\varepsilon_m}{\nu}\frac{1}{4QZ^{\frac{1}{2}}}\left[\frac{r}{r_e}\frac{\partial Z}{\partial R}\right]^2 - \frac{C_2}{Q}\frac{E^2}{Z^{\frac{1}{2}}} + \frac{\partial}{\partial R}\left[\left(\frac{r}{r_e}\right)^2 Z^{\frac{1}{2}}\left[1 + \frac{\varepsilon_m}{\nu\delta_\varepsilon}\right]\frac{\partial E}{\partial R}\right] \tag{9}$$

where C_1, C_2, δ_k, δ_ε are constants. Again axial diffusion terms are neglected.

The forms of these equations, which embody considerable simplification of their exact form, do not apply to the low turbulence Reynolds number region close to the wall. A simplified model for ε_m was used in the region near the wall $0 < y^+ < y_p^+$, which was based on the Van Driest hypothesis:

$$\frac{\varepsilon_m}{\nu} = [Ky(1 - \exp(y^+/26))]^2\left[\frac{\partial Z}{\partial R}\right]\frac{u_b^2}{2\nu^2}\frac{r}{r_e}. \tag{10}$$

In order to match the two turbulence models at $y^+ = y_p^+$ it is assumed that:

$$\left(\frac{\overline{u'v'}}{k}\right)_p = \sqrt{(C_m)}$$

where $\overline{u'v'}$ is obtained from the near wall solution of momentum with equation (10). This provides boundary values Q_p and E_p for the solution of equations (5), (6), (8) and (9) in the region $y^+ > y_p^+$.

Hence

$$Q_p = \frac{(\overline{u'v'})_p}{u_b^2\sqrt{(C_m)}}$$

and from equation (7)

$$E_p = \frac{C_m Q_p^2}{(\varepsilon_m/\nu)_p}.$$

The turbulent boundary-layer calculation was given initial laminar velocity and temperature profiles generated from flat inlet profiles. The turbulent boundary-layer solution began at a specified boundary-layer thickness Reynolds number and this was a constant for all the predictions. The inlet profiles for Q and E were assumed to be flat. The magnitude of Q at inlet was measured in the experiments and the same values were used in the calculations. The inlet value for E could not be measured directly, but measurements of axial variation of free stream turbulence kinetic energy near inlet yield an estimate of E. From equation (8)

$$E_{\text{in}} = -Z^{\frac{1}{2}}\frac{\partial Q}{\partial X}. \tag{11}$$

For the range of turbulence levels at inlet it was assumed that the corresponding dissipation rate could be correlated by the following expression:

$$E_{\text{in}} = C_3 Q_{\text{in}}^{3/2}. \tag{12}$$

Values of E_{in} were obtained from measurements of $\partial Q/\partial X$ and Z using equation (11). The value of C_3 was hence determined from equation (12) and equation (12) was used in the program. C_3 is an inverse Reynolds number based on a dissipation length scale. This was assumed to be proportional to the boundary-layer thickness Reynolds number at inlet and therefore C_3 is a constant.

The following constant values were used in all the predictions:

$C_1 = 1.44$	$\delta_K = 0.41$
$C_2 = 2.0$	$\delta_h = 0.9$
$C_3 = 2.34 \times 10^{-5}$	$\delta_k = 1.0$
$C_m = 0.07$	$\delta_\varepsilon = 1.3$

which were taken from Launder and Spalding [1].

Computation details

The governing equations were solved by a parabolic computation scheme based on the Crank–Nicholson method. The annular mass flow space was resolved by 92 cross stream nodes which were distributed in the form of a geometric progression in the radial direction. It was therefore possible to maintain good resolution near the walls where the slopes of the dependent variables are greatest. A typical run time on the UMRCC CDC 7600 was 60 s although a large proportion of this time was used in solving the flow near the entrance ($X/D_e < 1.0$). The step lengths in the axial direction were controlled so that the change in the pressure gradient correction was less than 10^{-3}.

6. RESULTS

The results to be discussed in this section are only a selection which are chosen having regard to the objectives of the experiment which were: (a) To provide data on the variation of mean flow parameters in the entrance region of an annular duct; (b) To test the success of a turbulence prediction method; (c) To investigate the influence of inlet turbulence level particularly by the inclusion of a turbulence promoter.

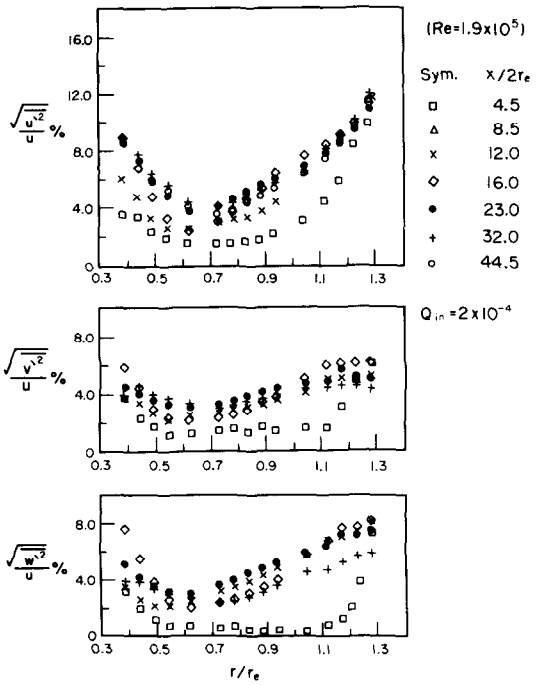

FIG. 2. Profiles of local turbulence levels (without turbulence promoter).

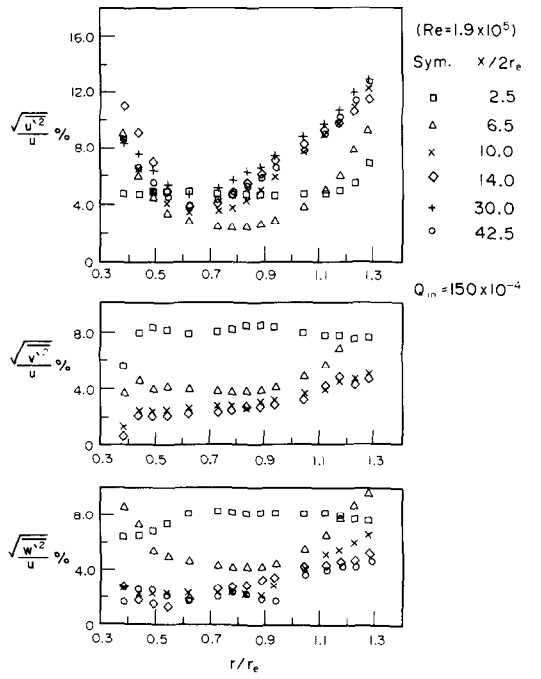

FIG. 3. Profiles of local turbulence levels (with turbulence promoter).

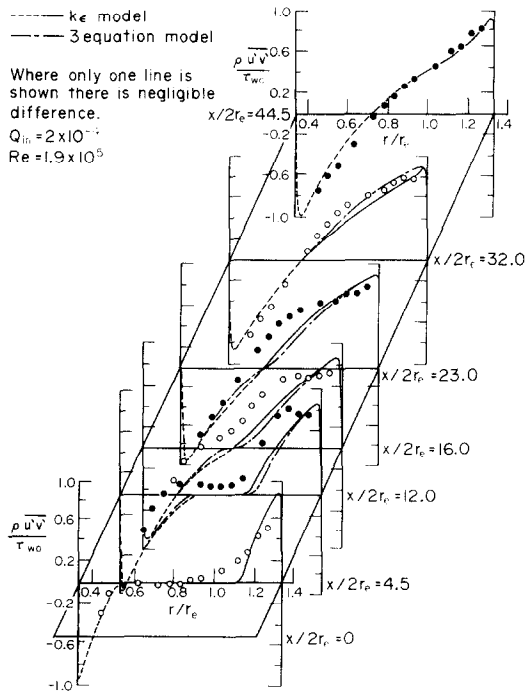

FIG. 4(a). Reynolds stress profiles along the annulus (without turbulence promoter).

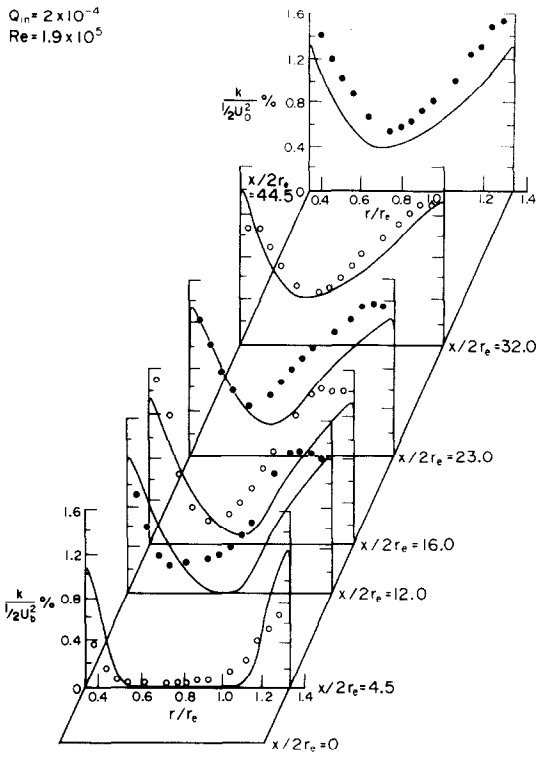

FIG. 5(a). Profiles of turbulence kinetic energy (without turbulence promoter).

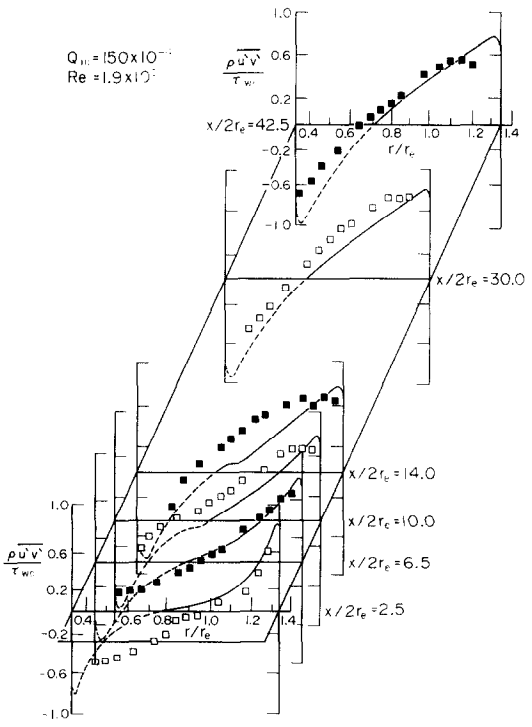

FIG. 4(b). Reynolds stress profiles along the annulus (with turbulence promoter).

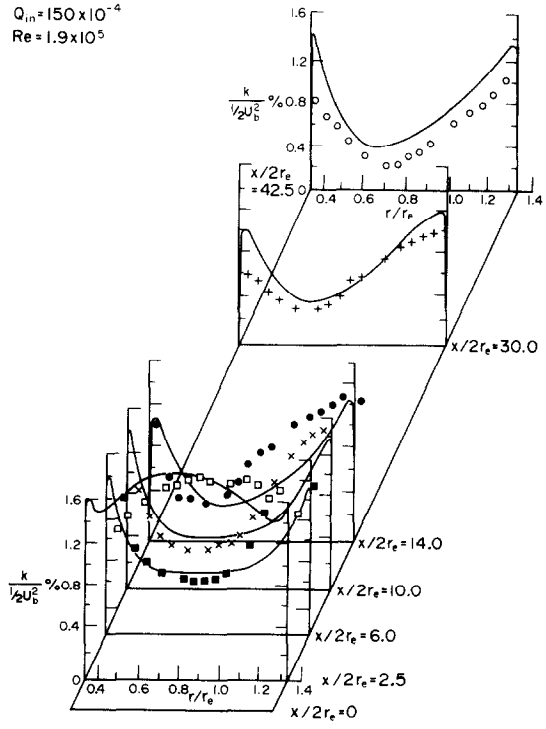

FIG. 5(b). Profiles of turbulence kinetic energy (with turbulence promoter).

The turbulence promoter was found to increase the inlet turbulence energy at the Reynolds number used by a factor of $\times 75$.

At 32 equivalent diameters there is no difference in the predictions for the two turbulence levels and the velocity profile has achieved its fully developed shape.

Figures 2 and 3 show the local turbulence levels in the three directions axial, radial and tangential. At a distance of the order of 12 equivalent diameters the boundary layers on each side have interfered and the turbulence levels do not show much change after this position. The effect of the turbulence promoter is, as would be expected, important in the early stages of the flow with very high turbulence levels in the central regions decaying rapidly along the duct.

Figures 4(a) and 4(b) show the shear stress profiles in an isometric form. It is clear that apart from the experimental errors the prediction is in good agreement with the experiment. Without the turbulence promoter there is a core region with zero Reynolds stress which persists until the boundary layers interfere but with the turbulence promoter included this region is very much reduced and is not apparent at the first measuring motion. The very high turbulence level at entrance will cause the Reynolds stress to diffuse more rapidly into the central regions. However, this situation of large difference from equilibrium does not appear to achieve the fully developed situation over any shorter distance than the normal situation. Also shown on Fig. 4(a) is the result of using the three equation turbulence model of Hanjalic and Launder [2]. It can be seen that there is only a small difference between the prediction of the two turbulence models as would be expected in this situation where the radial rate of diffusion of Reynolds stress is small. The corresponding changes in velocity profiles were also negligible. Figures 5(a) and 5(b) show comparisons of the turbulence energy. Whilst there is appreciable scatter the agreement is fairly good and again the prediction has successfully shown the very anomalous profile at the first station when the turbulence promoter is in position. A comparison at a lower Reynolds number but without turbulence promoter is shown on Fig. 6 with only the initial and final profiles shown for clarity. Figure 7 shows variations of inner and outer friction factors along the duct, the measured values being

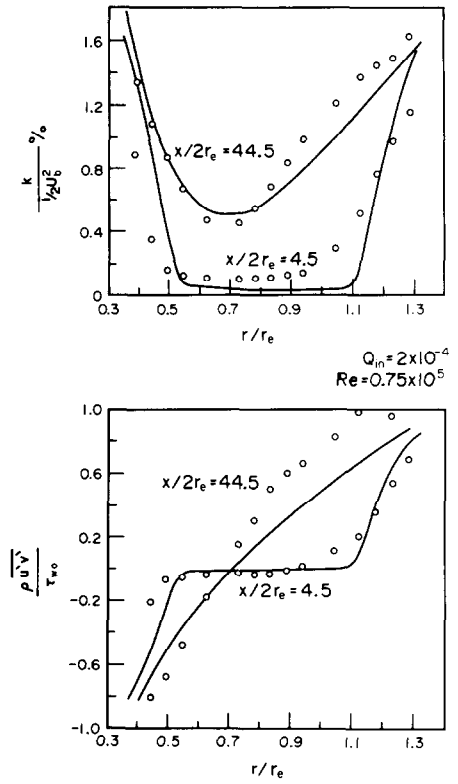

FIG. 6. Development of turbulence kinetic energy and Reynolds stress profiles.

obtained by Preston tube. Whilst some criticism has been made of this method for the inner friction factor, it has been shown to be reliable at the radius ratio used in this experiment. In the fully developed situation the total friction factor agreed well with the value obtained from the static pressure gradient. The fully developed value agreed with the accepted parallel wall correlation

$$C_f = 0.087 Re^{-\frac{1}{4}}.$$

The measured friction factors in the entrance region are somewhat higher than the calculated values but both measurements and predictions reflect the same trends, namely, the inner friction factor being higher than the outer and the increased turbulent energy

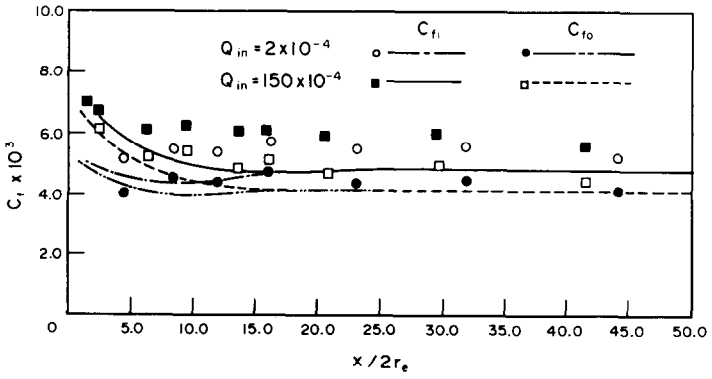

FIG. 7. Variation of the friction coefficients along the annulus.

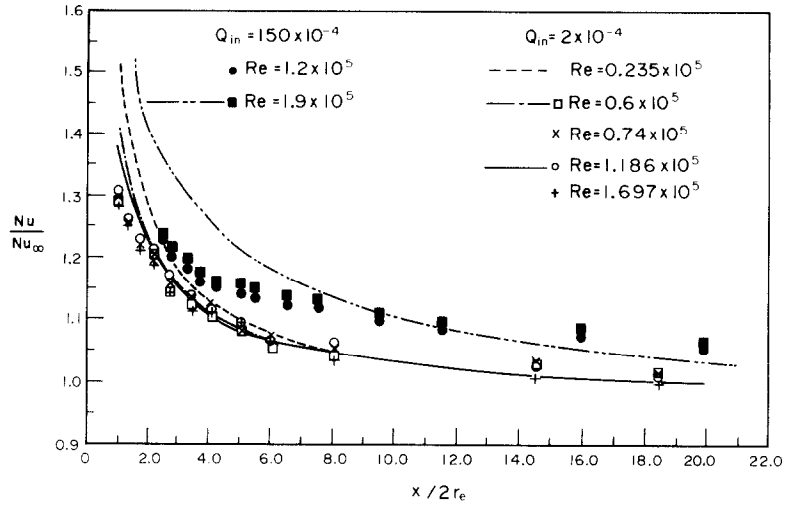

FIG. 8. Variation of Nusselt number along the annulus.

causing an increase in the initial region. The position of the radius of maximum velocity was in agreement with the empirical formula of Kays and Leung [6] which was obtained from a large number of experimental measurements by other workers.

Finally, Fig. 8 shows the variation of Nusselt number in the entrance region expressed as the ratio of the local to fully developed value. The prediction shows a marked increase of heat transfer in the entrance with the turbulence promoter present and the measurements also show this effect. However, close to the promoter the agreement is not good probably due to the difficulty of ensuring that the start of heating takes place at the promoter position. There is inevitably some conduction in the core which gives a small heat flux upstream of the nominal position of the start of heating. This effect will produce a reduction in heat transfer coefficient and is possibly the cause of the lack of agreement in the very early stages.

7. CONCLUSIONS

(1) Turbulence kinetic energy, shear stress, velocity and heat transfer have been measured in the flow development region of an annulus with two levels of free stream turbulence at inlet. The results agree well with a prediction method using the two equation model.

(2) The use of a turbulence promoter producing a 75 times enhancement of turbulence intensity at inlet was seen to produce an increase of friction and heat transfer in the entrance region. The length required to achieve the fully developed situation seemed to be unchanged.

(3) The measurements and predictions in the fully developed situation of friction, heat transfer and radius of maximum velocity were in good agreement and also agreed well with generally accepted values.

REFERENCES

1. B. E. Launder and D. B. Spalding, *Mathematical Models of Turbulence*. Academic Press, London (1972).
2. K. Hanjalic and B. E. Launder, A Reynolds stress model of turbulence and its application to thin shear flows, *J. Fluid Mech.* **52**, Part 4, 609–638 (1972).
3. S. L. Smith, C. J. Lawn and M. J. Hamlin, The direct measurement of wall shear in an annulus, CEGB Report RD/B/N1232 (1968).
4. J. A. Brighton and J. B. Jones, Fully developed turbulent flow in annuli, *J. Basic Engng* **86**, 835–844 (1964).
5. A. Quarmby and R. K. Anand, Turbulent heat transfer in the thermal entrance region of concentric annuli with uniform wall heat flux, *Int. J. Heat Mass Transfer* **13**, 395–411 (1970).
6. W. M. Kays and E. Y. Leung, Heat transfer in annular passages hydrodynamically developed turbulent flow with arbitrarily prescribed heat flux, *Int. J. Heat Mass Transfer* **6**, 537–557 (1963).
7. N. W. Wilson and J. O. Medwell, An analysis of heat transfer for fully developed turbulent flow in concentric annuli, *J. Heat Transfer* **90**, 43–50 (1968).
8. A. Roberts and H. Barrow, Turbulent heat transfer to air in the vicinity of the entry of an internally heated annulus, *Proc. Instn Mech. Engrs* **182**, Part 3H, 268–276 (1967).
9. P. L. Stephenson, A theoretical study of heat transfer in two-dimensional turbulent flow in a circular pipe and between parallel and diverging plates, *Int. J. Heat Mass Transfer* **19**, 413–423 (1976).
10. A. P. Hatton and N. H. Woolley, Heat transfer in two-dimensional turbulent confined flows, *Proc. Instn Mech. Engrs* **186**, 625–633 (1972).
11. P. Walklate, M. R. F. Heikal and A. P. Hatton, Measurement and prediction of turbulence and heat transfer in the entrance region of a pipe. To be published.
12. T. W. Davies and M. A. Patrick, A simplified method of improving the accuracy of hot-wire anemometry, DISA Conference, pp. 152–155 (1972).
13. F. H. Champagne and C. A. Sleicher, Turbulence measurements with inclined hot-wires, Part 2: Hot wire response equations, *J. Fluid Mech.* **28**, Part 1, 177–182 (1967).
14. R. W. Briley, Numerical method for predicting three-dimensional steady viscous flow in ducts, *J. Comput. Phys.* **14**, 8 (1974).

EFFET DU NIVEAU DE TURBULENCE INCIDENT SUR L'ECOULEMENT ET LE TRANSFERT THERMIQUE DANS LA REGION D'ENTREE D'UN ESPACE ANNULAIRE

Résumé—On présente les mesures faites sur les caractéristiques de la turbulence, sur les paramètres de l'écoulement moyen et du transfert thermique à l'entrée d'un espace annulaire dont le rapport des rayons est égal à 0,25, pour un domaine de nombres de Reynolds allant de $0{,}13 \times 10^5$ à $1{,}9 \times 10^5$. Des essais ont été menés avec ou sans promoteur de turbulence, lequel donne un fort accroissement de turbulence dans l'écoulement libre à l'entrée. On compare les résultats avec le calcul à partir du modèle à deux équations de turbulence. Un bon accord est obtenu à la fois pour la région d'entrée et pour la région de régime établi et aussi avec ou sans le promoteur de turbulence, à condition de considérer les valeurs convenables de l'énergie de la turbulence initiale et de la dissipation.

DER EINFLUSS DES FREISTRAHL-TURBULENZNIVEAUS AUF DIE STRÖMUNG UND DEN WÄRMEÜBERGANG IM EINLAUFBEREICH EINES RINGKANALS

Zusammenfassung—Im Einlaufbereich eines Ringkanals mit einem Radienverhältnis von 0,25 wurden für $0{,}13 \times 10^5 < Re < 1{,}9 \times 10^5$ die Turbulenzgrößen, die Strömungs- und die Wärmeübergangs-Parameter gemessen. Die Versuche wurden mit und ohne Turbulenzpromotoren durchgeführt; letztere ergaben eine starke Erhöhung der Freistrahlturbulenz im Eintritt. Die Ergebnisse wurden mit der auf dem Zwei-Gleichungs-Turbulenzmodell basierenden Berechnungsmethode verglichen. Sowohl für den Einlaufbereich wie für die voll ausgebildete Strömung, mit und ohne Turbulenzpromotoren, ergab sich eine gute Übereinstimmung, vorausgesetzt, es wurden geeignete Werte für die anfängliche Turbulenzenergie und die Dissipationsrate verwendet.

ВЛИЯНИЕ УРОВНЯ ТУРБУЛЕНТНОСТИ ВНЕШНЕГО ПОТОКА НА ТЕЧЕНИЕ И ТЕПЛООБМЕН ВО ВХОДНОЙ ОБЛАСТИ КОЛЬЦЕВОГО КАНАЛА

Аннотация — Проведены измерения характеристик турбулентности, параметров среднего течения и переноса тепла во входной области кольцевого канала с отношением радиусов 0,25 в диапазоне чисел Рейнольдса от $0{,}13 \cdot 10^5$ до $1{,}9 \cdot 10^5$. Опыты проводились как с турбулизатором, который значительно усиливал турбулентность основного потока на входе, так и без него. Экспериментальные данные сравнивались с результатами численного счета, полученными с помощью модели турбулентности, состоящей из двух уравнений. Подбор подходящих значений начальной энергии турбулентности и скорости диссипации позволил получить хорошее соответствие сравниваемых результатов как для входного участка, так и для полностью установившегося течения.